Behavioral assessment of sensitivity to intracortical microstimulation of primate somatosensory cortex

Sungshin Kim[a], Thierri Callier[a], Gregg A. Tabot[b], Robert A. Gaunt[c], Francesco V. Tenore[d], and Sliman J. Bensmaia[a,b,1]

[a]Department of Organismal Biology and Anatomy, University of Chicago, Chicago, IL 60637; [b]Committee on Computational Neuroscience, University of Chicago, Chicago, IL 60637; [c]Department of Physical Medicine and Rehabilitation, University of Pittsburgh, Pittsburgh, PA 15213; and [d]Research and Exploratory Development Department, Applied Physics Laboratory, Johns Hopkins University, Laurel, MD 20723

Edited by Ranulfo Romo, Universidad Nacional Autonóma de México, Mexico City, D.F., Mexico, and approved September 29, 2015 (received for review May 13, 2015)

Intracortical microstimulation (ICMS) is a powerful tool to investigate the functional role of neural circuits and may provide a means to restore sensation for patients for whom peripheral stimulation is not an option. In a series of psychophysical experiments with nonhuman primates, we investigate how stimulation parameters affect behavioral sensitivity to ICMS. Specifically, we deliver ICMS to primary somatosensory cortex through chronically implanted electrode arrays across a wide range of stimulation regimes. First, we investigate how the detectability of ICMS depends on stimulation parameters, including pulse width, frequency, amplitude, and pulse train duration. Then, we characterize the degree to which ICMS pulse trains that differ in amplitude lead to discriminable percepts across the range of perceptible and safe amplitudes. We also investigate how discriminability of pulse amplitude is modulated by other stimulation parameters—namely, frequency and duration. Perceptual judgments obtained across these various conditions will inform the design of stimulation regimes for neuroscience and neuroengineering applications.

neuroprosthetics | psychophysics | brain–machine interfaces | threshold | just noticeable difference

Intracortical microstimulation (ICMS) is an important tool to investigate the functional role of neural circuits (1, 2). In a famous example, microstimulation of neurons in the middle temporal area was found to bias the perceived direction of visual motion stimuli, causally implicating these neurons in the computation of visual motion direction (3). Experiments with ICMS of somatosensory cortex showed that changing the frequency of stimulation elicited discriminable percepts, demonstrating that temporal patterning of cortical responses has perceptual correlates (4). Building on the success of these and other studies, ICMS has been proposed as an approach to restore perception in individuals who have lost it, for example in visual neuroprostheses for the blind (5, 6) or somatosensory neuroprostheses for tetraplegic patients (7–11). In the present study, we sought to characterize the psychometric properties of ICMS delivered to primary somatosensory cortex (S1) across a wide range of stimulation regimes. In psychophysical experiments with Rhesus macaques, we first measured the detectability of ICMS pulse trains and assessed its dependence on a variety of stimulation parameters. We then measured the degree to which animals could discriminate pairs of ICMS pulse trains that differed in amplitude. In both the detection and discrimination experiments, ICMS parameters—amplitude, pulse width, pulse train duration, and pulse train frequency—spanned the range that is detectable and has been typically deemed safe (12–14). Results from the present experiments will inform the design of future studies involving ICMS as well as the development of sensory encoding algorithms for neuroprostheses.

Results

We trained two monkeys to perform two variants of a two-alternative forced-choice (2AFC) task: a detection task and a discrimination task. In both tasks, the animal was seated in front of a computer monitor that conveyed information about the trial progression (Fig. 1 *A* and *B*). Each trial consisted of two successive stimulus intervals, each lasting 1 s and indicated by the appearance of a circle on a visual monitor, separated by a 1-s interstimulus interval during which the circle disappeared (Fig. 1*B*). In the detection task, the animal indicated which of the two intervals contained the stimulus by making a saccade to a left or a right target. In the discrimination task, the animal indicated which of two intervals contained the more intense stimulus by making a saccade to a left or a right target.

ICMS was delivered through a Utah electrode array (UEA; Blackrock Microsystems Inc.) implanted in the hand representation of area 1 and a floating microelectrode array (FMA; Microprobes for Life Science) in the hand representation of area 3b (Fig. 1 *C* and *D*). UEAs comprise 96 electrodes, 1.5 mm in length and spaced 400 μm apart, with tips coated with an iridium oxide film, and the FMAs comprise 16 electrodes, 3 mm in length and spaced 1.2 mm apart, with tips coated with an activated iridium film. ICMS consisted of symmetrical biphasic pulse trains delivered through a 96-channel constant-current neurostimulator (CereStim R96; Blackrock Microsystems Inc.).

Detection. In addition to pulse amplitude, several stimulation parameters are known to affect the detectability of ICMS, including (but not limited to) pulse width, pulse frequency, and pulse train duration. As might be expected, increases in all three of those parameters led to higher sensitivity, as evidenced by leftward shifts in the psychometric functions and lower detection thresholds, defined as the current amplitude required to achieve 75% correct

Significance

Electrical stimulation of sensory structures in the brain is a powerful tool to investigate neural circuits and may provide a means to restore sensation for patients for whom stimulation of the nerve is not an option. For both purposes, however, it is critical to understand how the design of the stimulation shapes the evoked sensory experience. With this in mind, we investigate the ability of monkeys to detect and discriminate trains of electrical pulses delivered to their somatosensory cortex through chronically implanted electrode arrays. We show that artificial touch is highly dependent on various features of the electrical stimuli and discuss the implications of our results for the use of electrical stimulation in neuroscience and neural engineering.

Author contributions: R.A.G., F.V.T., and S.J.B. designed research; T.C. performed research; S.K. and G.A.T. analyzed data; and S.K., T.C., G.A.T., R.A.G., F.V.T., and S.J.B. wrote the paper.

The authors declare no conflict of interest.

This article is a PNAS Direct Submission.

Freely available online through the PNAS open access option.

See Commentary on page 15012.

[1]To whom correspondence should be addressed. Email: sliman@uchicago.edu.

This article contains supporting information online at www.pnas.org/lookup/suppl/doi:10.1073/pnas.1509265112/-/DCSupplemental.

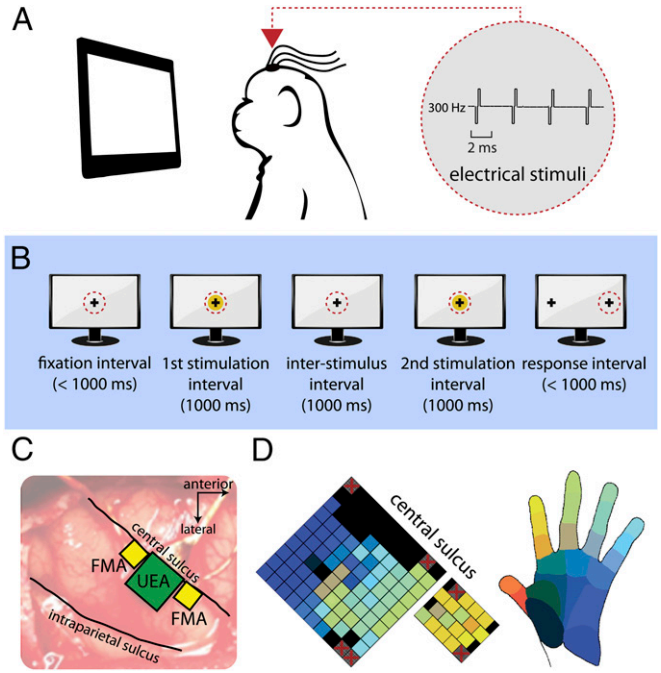

Fig. 1. Experimental design. (*A*) Experimental setup. (*Inset*) Temporal profile of ICMS pulse trains. (*B*) Trial structure in the two-alternative forced-choice tasks. The red-dotted circle denotes the animal's point of gaze. (*C*) Chronically implanted electrode arrays for one of the two monkeys: one UEA was implanted in area 1 (green) and two FMAs were implanted in area 3b (yellow). (*D*) The UEA and the anterolateral FMA impinged on the hand representation in S1 (the other FMA impinged on the proximal limb representation and therefore was not used in the behavioral experiments).

performance on the task (Fig. 2 *A*–*C*). First, for 1-s-long, 300-Hz ICMS, increases in pulse width (from 50 to 400 μs) led to significant decreases in detection threshold [Fig. 2*A*, Friedman test, $\chi^2(3, 21) = 22.95$, $P < 10^{-4}$] as might be expected given that wider pulses lead to higher charge injection (in the cathodic phase) when other stimulation parameters are held constant. However, significantly more charge was required to reach threshold for longer phases [Fig. 3*A*, Friedman test, $\chi^2(3, 21) = 18.45$, $P < 0.001$], which likely reflects a progressive increase in sodium inactivation (15).

Second, with all other parameters held constant, detection thresholds also decreased significantly as ICMS frequency increased but leveled off at 250 Hz [Fig. 2*B*, Friedman test, $\chi^2(4, 44) = 37.27$, $P < 10^{-6}$]. Interestingly, the range over which increases in frequency lead to improved detection performance is considerably wider for primate somatosensory cortex than for rodent auditory cortex, where thresholds level off at 80 Hz (16).

Third, we found that detection thresholds decreased as pulse train duration increased, leveling off at ∼200 ms [Fig. 2*C*, Friedman test, $\chi^2(3, 9) = 10.2$, $P < 0.05$], as we (and others) have previously reported (8). In other words, if a stimulation regime is imperceptible after 200 ms, it will remain so no matter what its duration, which sheds light on the time course over which ICMS is integrated for detection.

Fourth, we wished to determine the degree to which the observed increase in sensitivity with increases in frequency simply reflected the concomitant increase in the total number of pulses delivered (17, 18). To this end, we had the animals perform the detection task with pulse trains that varied in both frequency and duration, with other parameters held constant (Fig. 2*D*). We found that detection performance was dependent on both frequency and duration. On the one hand, the duration to achieve criterion performance significantly decreased as frequency increased [Friedman test, $\chi^2(4, 24) = 26.63$, $P < 10^{-4}$]. On the other hand, the number of pulses required to reach threshold significantly increased as frequency increased beyond 100 Hz [Fig. 3*B*, Friedman test, $\chi^2(4, 24) = 23.89$, $P < 10^{-4}$]. In other words, sensitivity was not completely determined by the number of pulses delivered: fewer pulses were required to achieve threshold at low frequencies.

Finally, we investigated whether pulse width and frequency interact in determining detectability. We found that, though thresholds (expressed in charge per phase) were lower for short pulses, this difference disappeared at high frequencies (Fig. 3*C*).

In summary, the lowest thresholds, as measured in current amplitude, are achieved with long pulse widths and higher frequencies (Fig. 2 *A* and *B*). However, the most efficient stimulation in terms of threshold charge is achieved with short pulses and low frequencies (Fig. 3 *A* and *B*).

Overall, thresholds reported here were largely overlapping with those obtained in previous studies (19). In one study investigating detection of ICMS of S1 (targeting primarily area 2), detection thresholds were found to range from 5 to 40 μA (20). In primary visual cortex, detection thresholds typically range from 5 to 15 μA, and thresholds have been found to be relatively consistent across visual areas (21).

Discrimination. To fully characterize the perceptual properties of ICMS, we need to measure not only how detectable pulses are, but also how discriminable they are from one another. Romo et al. (4) showed, in a landmark study, that primates could distinguish changes in ICMS frequency, which ostensibly were associated with changes in the perceived frequency of artificial tactile flutter (22). Here, we sought to estimate the degree to which primates could distinguish changes in ICMS amplitude, which are associated with changes in perceived intensity (8). To this end, we had animals perform an amplitude discrimination task in a 2AFC paradigm (Fig. 1*B*), from just above detection threshold (30 μA) to 100 μA (12, 14). We then estimated the just noticeable differences (JNDs) from their performance on the task (based on a criterion of 75% correct performance). Furthermore, we assessed the dependence of JNDs on two other stimulation parameters—namely, ICMS frequency and duration (Fig. 4).

First, we found that JNDs obtained from areas 3b and 1 were indistinguishable [with matched polarity, in this case anodal, $t(30) = 0.400$, $P = 0.692$], as we have shown detection thresholds to be (8).

Second, JNDs were relatively constant over the range of amplitudes tested (Fig. 4*A*). Trials with the 30-μA and 100-μA standards, run with anodal phase-leading pulses, were interleaved in the same experimental blocks using the same set of electrodes (eight each in areas 1 and 3b) and yielded statistically indistinguishable JNDs (signed rank test, $P = 0.278$). JNDs obtained with the 70-μA standard, run with cathodal phase-leading stimulation, were significantly lower than those measured with the 30- and 100-μA standards [$t(39) = 2.44$, $P = 0.02$], as might be expected given that cathodal phase-leading stimulation yields better sensitivity (16, 23). In fact, detection thresholds with cathodal and anodal phase-leading stimulation differ on average by ∼10 μA, which matches the observed difference in JNDs between the 70- and 30/100-μA standards.

Third, in contrast to detection, discrimination performance was largely independent of stimulus frequency [Fig. 4*B*, Friedman test, $\chi^2(3,24) = 6.73$, $P = 0.08$].

Fourth, discrimination performance improved as stimulus duration increased (Fig. 4*C*), leveling off at durations of ∼300 ms. Thus, ICMS seems to be integrated over slightly longer time scales for discrimination than for detection (cf. Fig. 2*C*). Similar time scales have been observed in a tactile discrimination task (24), suggesting that information about artificial touch is integrated over a similar time scale as is information about natural touch (25). Note that discrimination performance was near chance with 50-ms stimuli (Fig. 4*C*) because these were barely detectable (Fig. 2*D*).

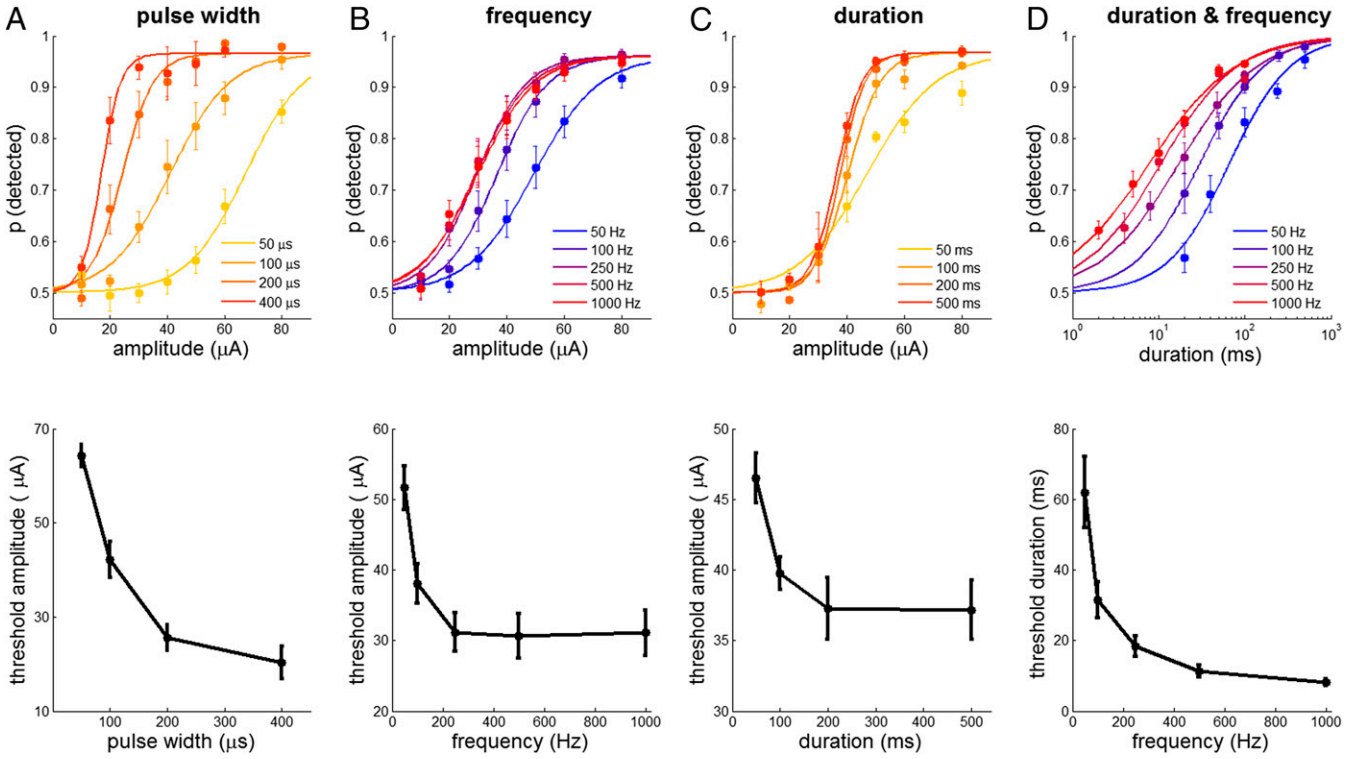

Fig. 2. Dependence of detectability on stimulation parameters. (*A*) Pulse width (28,126 trials from 13 electrodes). (*B*) Pulse train frequency (47,497 trials from 12 electrodes). (*C*) Pulse train duration (13,337 trials from four electrodes). (*D*) Pulse train duration and frequency (21,198 trials from 12 electrodes). ICMS amplitude was 40 μA.

Discussion

Constancy of JNDs. JNDs were approximately constant over the range of standard amplitudes tested, which stands in contrast to what is observed with natural stimulation of peripheral receptors across all modalities. Indeed, natural sensory modalities approximately obey Weber's law, which states that JNDs will increase linearly with increases in standard amplitude (26). As originally formalized by Johnson (27, 28), the relationship between JNDs and standard amplitude is determined by the rate–intensity function, which describes how the mean response rate of the activated neuronal population changes as the amplitude changes, and the variance–rate function, which describes how the response variance changes as the mean rate changes (29, 30). If these two functions are described as power functions with exponents p and q, respectively, the JND should be related to the standard amplitude I according to the following equation (29, 30):

$$JND \propto I^{\omega}, \quad [1]$$

where

$$\omega = 1 - p + pq/2. \quad [2]$$

With natural input (namely, mechanical stimulation of the hand), rate is a decelerating function of amplitude ($0 < P < 1$) (31, 32), whereas the variance is approximately linear with rate given Poisson firing ($q \sim 1$), which leads to the observed increase in JNDs with standard amplitude. Our results imply a different relationship between p and q, one that leads to a ω that is ~0, suggesting that p is greater than q. In other words, our behavioral

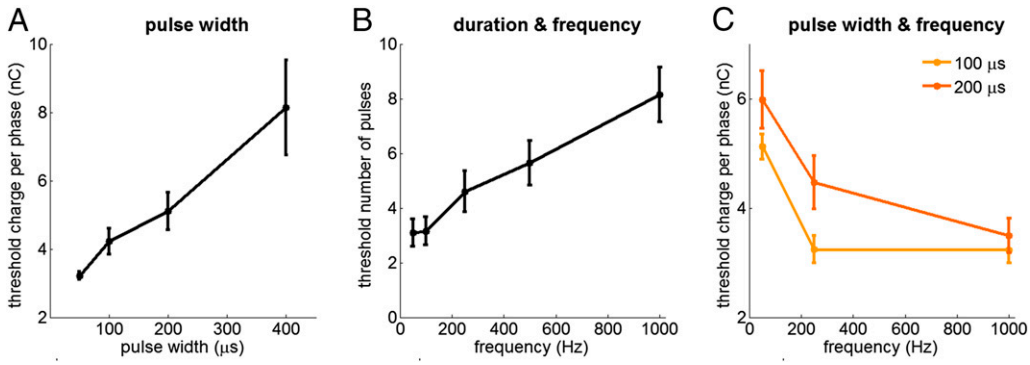

Fig. 3. (*A*) Threshold charge per phase from the pulse width manipulation. (*B*) Threshold number of pulses from the duration and frequency manipulation. (*C*) Threshold charge per phase from the pulse width and frequency manipulation.

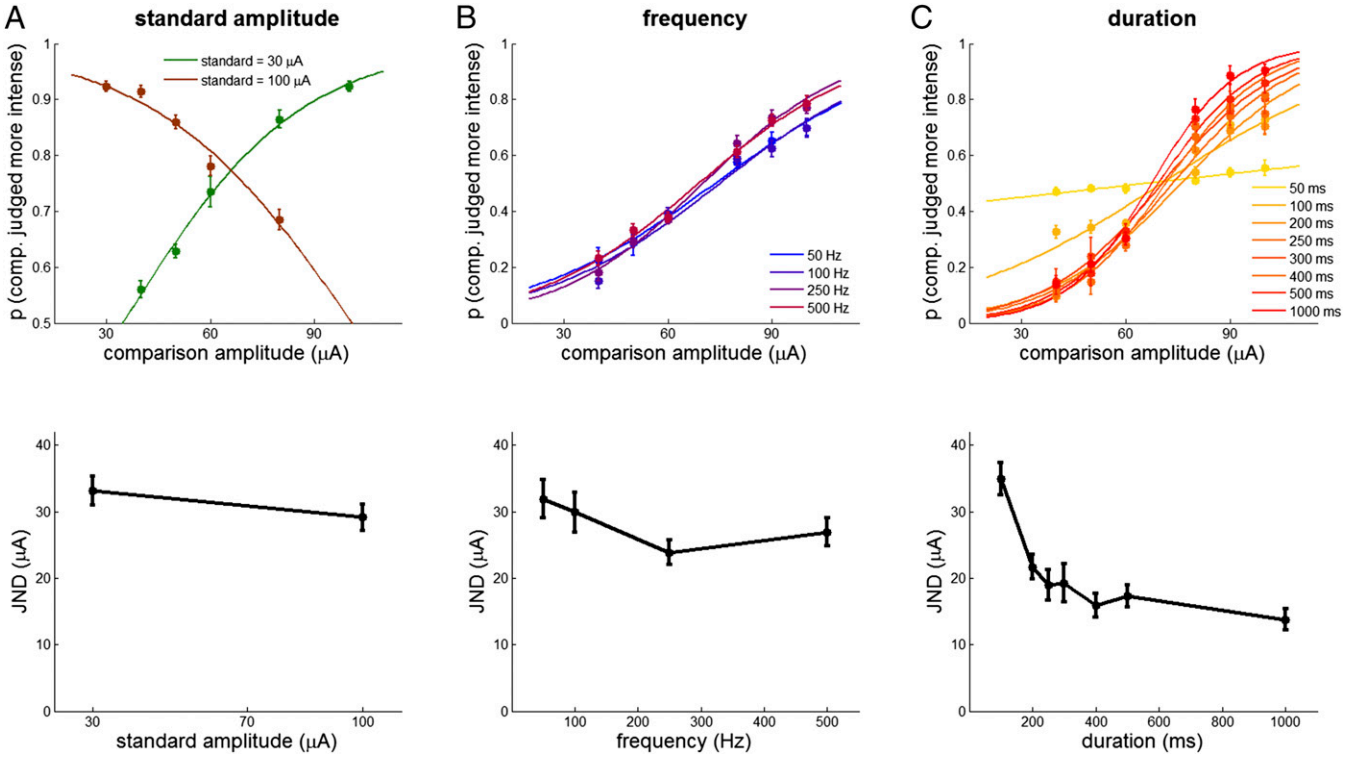

Fig. 4. Dependence of discriminability on stimulation parameters. (*A*) JND as a function of standard amplitude (20,052 trials from 16 electrodes). ICMS is at 300 Hz. (*B*) JND as a function of pulse train frequency, with a 70-μA standard (15,295 trials from nine electrodes). (*C*) JND as a function of pulse train duration, with a 70-μA standard (17,307 trials from nine electrodes).

results suggest that the interrelationships among stimulus amplitude, population firing rate, and neuronal noise are fundamentally different with natural and electrical stimulation, a prediction that can be validated once reliable measurements of ICMS-evoked population firing rates can be obtained.

Effects of Frequency. That changes in pulse frequency had little impact on amplitude discrimination does not imply that changes in this parameter do not have sensory consequences. In fact, increases in frequency likely cause two perceptual changes: an increase in perceived magnitude and one in perceived frequency (33). The impact on perceived magnitude is evident from the detection experiments, which showed that animals are more sensitive at higher frequencies. Though we did not test whether changes in frequency actually cause a change in perceived magnitude, results from experiments with rats (34) suggest that they do. The qualitative sensory consequences of changes in frequency were demonstrated in experiments that showed that monkeys that were trained to discriminate the frequency of skin vibrations could discriminate pulse frequency with frequencies below 50 Hz (4). Whether changes in ICMS frequency are discriminable at higher frequencies remains to be determined. However, some evidence suggests that the frequency of skin vibrations is encoded in the phase-locked responses of a subset of S1 neurons up to at least 800 Hz (31). The elicitation of phase-locked responses through ICMS, at least in this subpopulation of neurons, might thus result in an oscillatory percept the frequency of which will be determined by pulse frequency (as is the case with low-frequency ICMS).

At first glance, it may be surprising that ICMS thresholds decrease with frequency over a wider range in somatosensory cortex (up to ~250 Hz) than in auditory cortex (up to 80 Hz) (16) given the much wider bandwidth of audition relative to touch. However, though the basic structure of these two sensory cortices is similar (35), differences in their microcircuitry have been reported (36, 37). Furthermore, rodents can more readily detect very short asynchronies in ICMS pulses (delivered through two electrodes) when these are delivered to somatosensory cortex than to auditory cortex (38), suggesting that somatosensory cortex is more sensitive than auditory cortex to small differences in neural timing (on the order of 1–3 ms). Though they reflect a different aspect of perception, our findings are generally consistent with these previous neurophysiological and behavioral findings.

In the experiments described here, stimuli consisted of periodic pulse trains, which evoke unnaturally regular and periodic responses in the activated neuronal populations. Some evidence suggests that mimicking natural temporal patterns of activation through ICMS may be more efficient at evoking percepts. For example, simply introducing irregularity in the pulse trains (while keeping their overall frequency constant) yields more detectable percepts, perhaps because irregular spiking is more biomimetic than regular spiking (39; but see ref. 40 for counterevidence). A compelling example of how biomimetic patterning might modulate the efficiency of ICMS is provided by Kimmel and Moore (41), who delivered stimulation to the frontal eye fields (FEF) and showed that pulse trains whose frequency ramps up—thereby more closely mimicking the natural activation of FEF neurons—are more effective at evoking saccades than flat, decelerating, or randomly varying ones. Nonetheless, when evaluating the effect of temporal patterning on detectability, it is important to assess the degree to which the differential efficiency of different temporal patterns can be attributed to fluctuations in frequency or whether it reflects a sensitivity to other aspects of the temporal patterning (33).

Implications for Neuroprosthetics. That mean JNDs hover around 30 μA suggests that only two perceptually discriminable steps are achievable over the range from 30 μA (approximate absolute threshold) to 100 μA (maximum amplitude used), and the number of steps decreases if lower ICMS frequencies are used, by virtue of the fact that absolute thresholds go up as frequency decreases

below about 250 Hz (Fig. 2*B*). The decision to cap stimulation amplitude at 100 μA was motivated by the finding that stimulation up to this amplitude has been shown to have a negligible effect on the electrode–tissue interface (12) or on the neuronal tissue itself (14). Whether higher currents can be safely used chronically remains to be tested, but extending the range of amplitude would be a straightforward way to increase the dynamic range of artificial touch. That two discriminable increments of amplitude are achievable between threshold and the maximum amplitude tested (100 μA) severely limits the ability to convey sensory information by modulating amplitude. The dynamic range might also be improved by delivering more biomimetic stimulation patterns (39, 41) or by delivering stimulation through multiple electrodes simultaneously (20, 42), both of which are liable to result in higher sensitivity.

One might ask what range of pressure levels two JNDs might span. In parallel psychophysical experiments, we trained animals to discriminate changes in indentation depth and found the psychometrically equivalent dynamic range for mechanical stimuli to be up to 1.5 mm for one animal and 2.5 mm for the other (8). This equivalence is by no means well-defined given the strong dependence of the perceived intensity (and thus perceived pressure) of skin indentations not just on the magnitude of the pressure but on its rate of change (43–45). However, this comparison provides an order of magnitude approximation that can be refined as more sophisticated models linking pressure and its derivatives to perceived intensity are developed. The mapping between pressure and perceived intensity could in principle be derived by combining models that characterize the relationship between perceived intensity and afferent responses (46) with models that simulate populations' responses to arbitrary spatiotemporal skin deformations (47–50). In any case, ignoring the dynamical component of mechanically induced sensations, peak ICMS-evoked sensations correspond to those evoked by 200–600 kPa exerted on the skin (estimated from ref. 51).

An important constraint on ICMS in bidirectional brain–machine interfaces is the need to decode motor signals from one neuronal population while simultaneously electrically stimulating another (7, 52). Electrical artifacts produced by the stimulation pulses, which degrade decoding performance, can be reduced but not completely eliminated. Thus, low-frequency stimulation, resulting in fewer artifacts, will lead to better decoding performance. It is therefore unfortunate that low-frequency ICMS results in substantially lower sensitivity. To mitigate this problem will require the development of hardware that minimizes the duration of the artifacts and of algorithms that compensate for them (53–55).

Materials and Methods

Animals and Implants. Procedures were approved by the University of Chicago Institutional Animal Care and Use Committee. Each of two male Rhesus macaques (Macaca mulatta) 6 y of age, ~10 kg in weight) was implanted with three electrode arrays: one UEA (Blackrock Microsystems) and two FMAs (MicroProbes for Life Science). The UEA, implanted in the hand representation of area 1, consists of 96 electrodes with 1.5-mm-long shanks, spaced 400 μm apart and spanning a 4 × 4-mm area. The electrode tips are coated with a sputtered iridium oxide film using a standard process (56, 57). The electrode shaft is insulated with Parylene C along its length, with the exception of the tip, which has a targeted exposure length of 50 μm. Electrode impedances were measured to be between 10 and 80 kΩ before implantation. The two FMAs were implanted flanking the UEA and impinged on area 3b. Each FMA spans a 2.5 × 1.95-mm area and consists of 16 iridium electrodes with 3-mm-long shanks spaced 400 μm apart and insulated with Parylene C along their length, with the exception of the tip, whose surface area was nominally identical to that of the UEAs and was coated with an activated iridium oxide film (58, 59). We had specified electrode lengths of 3 mm based on our previous experience that the distal digit representation in area 3b lies at that depth. We mapped the receptive field of each electrode by identifying which areas of skin evoked multiunit activity (monitored through speakers; Fig. 1*D*). That our receptive fields on the FMAs were exclusively cutaneous and located at or near the tip of the finger indicates that these electrodes were impinging on area 3b. Only the FMA that impinged on the hand representation was used in the stimulation experiments (the other, more medial and posterior one, impinged on the arm representation in both animals). Stimulation pulses were delivered using a 96-channel constant-current neurostimulator (CereStim R96; Blackrock Microsystems).

Behavioral Tasks. Animals were seated at the experimental table facing a monitor, which signaled the trial progression (Fig. 1*A*). Each trial comprised two successive stimulus intervals, each indicated by a circle on a video monitor, lasting 1 s, and separated by a 1-s interstimulus interval during which the circle disappeared (Fig. 1*B*). Animals responded by making saccadic eye movements toward a left or right target and were rewarded with water or juice for correct responses. Unless otherwise specified, pulse width was 200 μs, frequency was 300 Hz, and duration was 1 s. The interphase interval was always 53 μs, the minimum interphase delay achievable with the neurostimulator (see Table S1 for summary of experimental manipulations and respective sample sizes). Animals had been trained on mechanical versions of each task, with stimuli consisting of mechanical indentations of the skin, delivered with a custom-made stimulator that can be controlled with micron precision (8).

Detection. On each trial, ICMS was delivered in one of two consecutive stimulus intervals, and the animal's task was to indicate which interval contained the stimulus by making a saccade to one of two visual targets (Fig. 1 *A* and *B*). In different experimental blocks, we investigated the effects of pulse width (50–400 μs), frequency (50–1,000 Hz), and pulse train duration (2–1,000 ms) on the animals' ability to detect stimuli varying in amplitude. We also studied the interaction between frequency and duration by varying these two parameters while keeping the pulse amplitude fixed at 40 μA as well as the interaction between pulse width and frequency using the range of amplitudes. Polarity was cathodal phase-leading in experiments with the UEAs and anodal phase-leading in experiments with the FMAs. The difference in polarity is due to the timing of the experiments: Experiments with FMAs were carried out shortly before those with UEAs. We realized that the stimulation polarity was reversed relative to the standard (cathodal phase leading) and changed it for subsequent experiments. However, though sensitivity to anodal phase-leading pulses was lower than that with cathodal phase-leading pulses, polarity did not modulate any of the observed effects (Fig. S1). In other words, though thresholds were higher for anodal than for cathodal phase-leading ICMS, the dependence on the tested stimulation parameters was the same for both. Each manipulation was repeated with multiple electrodes to gauge the generality of our results. For each condition and electrode, we computed the detection threshold using 75% accuracy as a performance criterion.

Amplitude discrimination. On each trial, two ICMS pulse trains were presented sequentially, and the animals' task was to indicate which of the two was more intense. A standard stimulus, whose amplitude was either constant throughout the block or took on one of two values, was paired with a comparison that varied over a range. In one experiment, the standard amplitude was 30 or 100 μA, and comparisons ranged from 30 to 100 μA (excluding the standard amplitude). Trials with the 30- and 100-μA standards were interleaved so the animal would have to pay attention to both intervals to perform the task correctly. On these blocks, stimulation consisted of anodal phase-leading pulses. In another experiment, in which the standard amplitude was 70 μA, we varied ICMS frequency (from 50 to 500 Hz) or pulse train duration (from 50 to 1,000 ms). In those conditions, the frequency or duration was the same for both intervals but varied randomly from trial to trial. In these experiments, stimulation consisted of cathodal phase-leading pulses. For each condition and electrode, we computed the discrimination threshold (or JND) using 75% accuracy as our performance criterion. Conditions with the 70-μA standard yielded two estimates of the JND, corresponding to 25% and 75% of judgments of the comparison as more intense than the standard. These two estimates were averaged.

ACKNOWLEDGMENTS. We thank Mark Histed, John Maunsell, Joseph O'Doherty, and Jeffrey Yau for their helpful comments on a previous version of this manuscript. This work was supported by Defense Advanced Research Projects Agency Contract N66001-10-C-4056.

1. Histed MH, Ni AM, Maunsell JH (2013) Insights into cortical mechanisms of behavior from microstimulation experiments. *Prog Neurobiol* 103:115–130.
2. Doty RW (1969) Electrical stimulation of the brain in behavioral context. *Annu Rev Psychol* 20:289–320.
3. Salzman CD, Murasugi CM, Britten KH, Newsome WT (1992) Microstimulation in visual area MT: Effects on direction discrimination performance. *J Neurosci* 12(6):2331–2355.
4. Romo R, Hernández A, Zainos A, Brody CD, Lemus L (2000) Sensing without touching: Psychophysical performance based on cortical microstimulation. *Neuron* 26(1):273–278.

5. Schmidt EM, et al. (1996) Feasibility of a visual prosthesis for the blind based on intracortical microstimulation of the visual cortex. *Brain* 119(Pt 2):507.
6. Dobelle WH (2000) Artificial vision for the blind by connecting a television camera to the visual cortex. *ASAIO J* 46(1):3–9.
7. O'Doherty JE, et al. (2011) Active tactile exploration using a brain-machine-brain interface. *Nature* 479(7372):228–231.
8. Tabot GA, et al. (2013) Restoring the sense of touch with a prosthetic hand through a brain interface. *Proc Natl Acad Sci USA* 110(45):18279–18284.
9. Dadarlat MC, O'Doherty JE, Sabes PN (2015) A learning-based approach to artificial sensory feedback leads to optimal integration. *Nat Neurosci* 18(1):138–144.
10. London BM, Jordan LR, Jackson CR, Miller LE (2008) Electrical stimulation of the proprioceptive cortex (area 3a) used to instruct a behaving monkey. *IEEE Trans Neural Syst Rehabil Eng* 16(1):32–36.
11. Tabot GA, Kim SS, Winberry JE, Bensmaia SJ (2014) Restoring tactile and proprioceptive sensation through a brain interface. *Neurobiol Dis* S0969-9961(14)00260-5.
12. Chen KH, et al. (2014) The effect of chronic intracortical microstimulation on the electrode–tissue interface. *J Neural Eng* 11(2):026004.
13. Parker RA, Davis TS, House PA, Normann RA, Greger B (2011) The functional consequences of chronic, physiologically effective intracortical microstimulation. *Prog Brain Res* 194:145–165.
14. Rajan AT, et al. (2015) The effect of chronic intracortical microstimulation on neural tissue and fine motor behavior. *J Neural Eng* 12(6):06608.
15. Merrill DR, Bikson M, Jefferys JG (2005) Electrical stimulation of excitable tissue: Design of efficacious and safe protocols. *J Neurosci Methods* 141(2):171–198.
16. Koivuniemi AS, Otto KJ (2012) The depth, waveform and pulse rate for electrical microstimulation of the auditory cortex. *Conf Proc IEEE Eng Med Biol Soc* 2012: 2489–2492.
17. Butovas S, Schwarz C (2007) Detection psychophysics of intracortical microstimulation in rat primary somatosensory cortex. *Eur J Neurosci* 25(7):2161–2169.
18. Stüttgen MC, Schwarz C (2010) Integration of vibrotactile signals for whisker-related perception in rats is governed by short time constants: Comparison of neurometric and psychometric detection performance. *J Neurosci* 30(6):2060–2069.
19. Tehovnik EJ (1996) Electrical stimulation of neural tissue to evoke behavioral responses. *J Neurosci Methods* 65(1):1–17.
20. Zaaimi B, Ruiz-Torres R, Solla SA, Miller LE (2013) Multi-electrode stimulation in somatosensory cortex increases probability of detection. *J Neural Eng* 10(5):056013.
21. Murphey DK, Maunsell JH (2007) Behavioral detection of electrical microstimulation in different cortical visual areas. *Curr Biol* 17(10):862–867.
22. Romo R, Hernández A, Zainos A, Salinas E (1998) Somatosensory discrimination based on cortical microstimulation. *Nature* 392(6674):387–390.
23. Tehovnik EJ, Slocum WM (2003) Microstimulation of macaque V1 disrupts target selection: Effects of stimulation polarity. Exp Brain Res 148:233–237.
24. Luna R, Hernández A, Brody CD, Romo R (2005) Neural codes for perceptual discrimination in primary somatosensory cortex. *Nat Neurosci* 8(9):1210–1219.
25. Godlove JM, Whaite EO, Batista AP (2014) Comparing temporal aspects of visual, tactile, and microstimulation feedback for motor control. *J Neural Eng* 11(4):046025.
26. Ekman G (1959) Weber's law and related functions. *J Psychol* 47:343.
27. Johnson KO (1980) Sensory discrimination: Neural processes preceding discrimination decision. *J Neurophysiol* 43(6):1793–1815.
28. Johnson KO (1980) Sensory discrimination: Decision process. *J Neurophysiol* 43(6): 1771–1792.
29. Gorea A, Sagi D (2001) Disentangling signal from noise in visual contrast discrimination. *Nat Neurosci* 4(11):1146–1150.
30. Kontsevich LL, Chen CC, Tyler CW (2002) Separating the effects of response nonlinearity and internal noise psychophysically. *Vision Res* 42(14):1771–1784.
31. Harvey MA, Saal HP, Dammann JF, 3rd, Bensmaia SJ (2013) Multiplexing stimulus information through rate and temporal codes in primate somatosensory cortex. *PLoS Biol* 11(5):e1001558.
32. Mountcastle VB, Talbot WH, Sakata H, Hyvärinen J (1969) Cortical neuronal mechanisms in flutter-vibration studied in unanesthetized monkeys. Neuronal periodicity and frequency discrimination. *J Neurophysiol* 32(3):452–484.
33. O'Doherty JE, Lebedev MA, Li Z, Nicolelis MA (2012) Virtual active touch using randomly patterned intracortical microstimulation. IEEE Trans Neural Syst Rehabil Eng 20:85.
34. Fridman GY, Blair HT, Blaisdell AP, Judy JW (2010) Perceived intensity of somatosensory cortical electrical stimulation. Exp Brain Res 203(3):499–515.
35. Linden JF, Schreiner CE (2003) Columnar transformations in auditory cortex? A comparison to visual and somatosensory cortices. *Cereb Cortex* 13(1):83–89.
36. Gururangan SS, Sadovsky AJ, MacLean JN (2014) Analysis of graph invariants in functional neocortical circuitry reveals generalized features common to three areas of sensory cortex. *PLOS Comput Biol* 10(7):e1003710.
37. Sadovsky AJ, MacLean JN (2013) Scaling of topologically similar functional modules defines mouse primary auditory and somatosensory microcircuitry. *J Neurosci* 33(35): 14048–14060, 14060a.
38. Yang Y, Zador AM (2012) Differences in sensitivity to neural timing among cortical areas. *J Neurosci* 32(43):15142–15147.
39. Doron G, von Heimendahl M, Schlattmann P, Houweling AR, Brecht M (2014) Spiking irregularity and frequency modulate the behavioral report of single-neuron stimulation. *Neuron* 81(3):653–663.
40. Histed MH, Maunsell JH (2014) Cortical neural populations can guide behavior by integrating inputs linearly, independent of synchrony. *Proc Natl Acad Sci USA* 111(1): E178–E187.
41. Kimmel DL, Moore T (2007) Temporal patterning of saccadic eye movement signals. *J Neurosci* 27(29):7619–7630.
42. Kim S, Callier T, Tabot GA, Tenore FV, Bensmaia SJ (2015) Sensitivity to microstimulation of somatosensory cortex distributed over multiple electrodes. *Front Syst Neurosci* 9:47.
43. Poulos DA, et al. (1984) The neural signal for the intensity of a tactile stimulus. *J Neurosci* 4(8):2016–2024.
44. Mei J, et al. (1983) The neural signal for skin indentation depth. II. Steady indentations. *J Neurosci* 3(12):2652–2659.
45. Burgess PR, et al. (1983) The neural signal for skin indentation depth. I. Changing indentations. *J Neurosci* 3(8):1572–1585.
46. Muniak MA, Ray S, Hsiao SS, Dammann JF, Bensmaia SJ (2007) The neural coding of stimulus intensity: Linking the population response of mechanoreceptive afferents with psychophysical behavior. *J Neurosci* 27(43):11687–11699.
47. Dong Y, et al. (2013) A simple model of mechanotransduction in primate glabrous skin. *J Neurophysiol* 109(5):1350–1359.
48. Kim SS, Mihalas S, Russell A, Dong Y, Bensmaia SJ (2011) Does afferent heterogeneity matter in conveying tactile feedback through peripheral nerve stimulation? IEEE Trans Neural Syst Rehabil Eng 19(5):514–520.
49. Kim SS, Sripati AP, Bensmaia SJ (2010) Predicting the timing of spikes evoked by tactile stimulation of the hand. *J Neurophysiol* 104(3):1484–1496.
50. Sripati AP, Vogelstein RJ, Armiger RS, Russell AF, Bensmaia SJ (2009) Conveying tactile feedback in sensorized hand neuroprostheses using a biofidelic model of mechanotransduction. *IEEE Trans Biomed Circuits Syst* 3(6):398–404.
51. Gulati RJ, Srinivasan MA (1995) Human fingerpad under indentation: Static and dynamic force response. Proc ASME Bioeng*ineer* Conf 29:261–262.
52. Bensmaia SJ, Miller LE (2014) Restoring sensorimotor function through intracortical interfaces: Progress and looming challenges. *Nat Rev Neurosci* 15(5):313–325.
53. Kent AR, Grill WM (2012) Recording evoked potentials during deep brain stimulation: Development and validation of instrumentation to suppress the stimulus artefact. *J Neural Eng* 9(3):036004.
54. Kent AR, et al. (2015) Measurement of evoked potentials during thalamic deep brain stimulation. Brain Stimul 8(1):42–56.
55. O'Doherty JE, Sabes PN (2014) Mitigating electrical stimulation artifacts for bidirectional neural interfaces. Program No. 444.06. *Neuroscience 2014 Abstracts* (Society for Neuroscience, Washington, DC). Available at abstractsonline.com/Plan/ViewAbstract.aspx?sKey=a98d1d55-f690-4bc5-a912-dbc4fb5dbdfa&cKey=9606415f-5b94-4820-b819-42521871ac5e&mKey=54c85d94-6d69-4b09-afaa-502c0e680ca7. Accessed October 13, 2015.
56. Negi S, Bhandari R, Rieth L, Solzbacher F (2010) In vitro comparison of sputtered iridium oxide and platinum-coated neural implantable microelectrode arrays. *Biomed Mater* 5(1):15007.
57. Negi S, Bhandari R, Rieth L, Van Wagenen R, Solzbacher F (2010) Neural electrode degradation from continuous electrical stimulation: Comparison of sputtered and activated iridium oxide. *J Neurosci Methods* 186(1):8–17.
58. Cogan SF, Troyk PR, Ehrlich J, Plante TD (2005) In vitro comparison of the charge-injection limits of activated iridium oxide (AIROF) and platinum-iridium microelectrodes. *IEEE Trans Biomed Eng* 52(9):1612–1614.
59. Musallam S, Bak MJ, Troyk PR, Andersen RA (2007) A floating metal microelectrode array for chronic implantation. *J Neurosci Methods* 160(1):122–127.